Chemistry–A European Journal
Research Article
doi.org/10.1002/chem.202202698
Chemistry Europe
European Chemical Societies Publishing
www.chemeurj.org

Light-Responsive Oligothiophenes Incorporating Photochromic Torsional Switches

Augustina Jozeliūnaitė,[a, b] Aiman Rahmanudin,[c] Saulius Gražulis,[d] Emilie Baudat,[e] Kevin Sivula,[c] Daniele Fazzi,*[f] Edvinas Orentas,*[b] and Giuseppe Sforazzini*[a, g]

Abstract: We present a quaterthiophene and sexithiophene that can reversibly change their effective π-conjugation length through photoexcitation. The reported compounds make use of light-responsive molecular actuators consisting of an azobenzene attached to a bithiophene unit by both direct and linker-assisted bonding. Upon exposure to 350 nm light, the azobenzene undergoes *trans*-to-*cis* isomerization, thus mechanically inducing the oligothiophene to assume a planar conformation (extended π-conjugation). Exposure to 254 nm wavelength promotes azobenzene *cis*-to-*trans* isomerization, forcing the thiophenic backbones to twist out of planarity (confined π-conjugation). Twisted conformations are also reached by *cis*-to-*trans* thermal relaxation at a rate that increases proportionally with the conjugation length of the oligothiophene moiety. The molecular conformations of quaterthiophene and sexithiophene were characterized by using steady-state UV-vis spectroscopy, X-ray crystallography and quantum-chemical modeling. Finally, we tested the proposed light-responsive oligothiophenes in field-effect transistors to probe the photo-induced tuning of their electronic properties.

Introduction

Conjugated compounds have been widely investigated as active components in numerous optoelectronic applications including light-emitting diodes,[1–5] solar cells,[6–9] field-effect transistors,[10–13] lasers,[14–17] and sensors.[18–22] Continuous efforts in the development of smart molecular design with thoughtful structure–property relationships, and control of the intermolecular interactions in the bulk, have allowed this class of molecules to reach unprecedented diffusion into commercial applications, for example, OLED screens and automotive lighting. A common approach to tuning the optical and electronic properties of conjugated compounds is by the functionalization of the π-system with electron-releasing or electron-withdrawing substituents.[23,24] At the same time, it is well known that these properties strongly depend on the geometry of the π-system. Thus, varying the regioregularity or tuning the steric interactions of lateral substituents are also the most common strategies used to tailor the physical properties of conjugated systems.[24–29] The strong optical response induced by twisting the π-system has been successfully applied, for instance, in thiophene derivatives for ion[19–20] and viscosity sensing.[30–32] The use of chemical triggers to tune the effective conjugation length of π-systems, however, is not compatible with the environmental insulation of optoelectronic devices that is necessary for their correct functioning and good lifetime.[33]

[a] *Dr. A. Jozeliūnaitė, Dr. G. Sforazzini*
Laboratory of Macromolecular and Organic Materials
Institute of Material Science and Engineering
Ecole Polytechnique Federale de Lausanne (EPFL)
1015 Lausanne (Switzerland)

[b] *Dr. A. Jozeliūnaitė, Prof. E. Orentas*
Department of Organic Chemistry
Faculty of Chemistry and Geosciences, Vilnius University
Naugarduko 24, LT-0325 Vilnius (Lithuania)
E-mail: edvinas.orentas@chf.vu.lt

[c] *Dr. A. Rahmanudin, Prof. K. Sivula*
Laboratory for Molecular Engineering of Optoelectronic Nanomaterials
Institute of Chemical Sciences and Engineering
Ecole Polytechnique Federale de Lausanne (EPFL)
1015 Lausanne (Switzerland)

[d] *Dr. S. Gražulis*
Vilnius University, Institute of Biotechnology
Saulėtekio al. 7, LT-10257 Vilnius (Lithuania)

[e] *E. Baudat*
Institute of Chemical Sciences and Engineering
Ecole Polytechnique Federale de Lausanne (EPFL)
1015 Lausanne (Switzerland)

[f] *Dr. D. Fazzi*
Dipartimento di Chimica "Giacomo Ciamician"
Università di Bologna
Via F. Selmi, 2, 40126 Bologna (Italy)
E-mail: daniele.fazzi@unibo.it

[g] *Dr. G. Sforazzini*
Present address:
Department of Chemical and Geological Sciences
University degli Studi di Cagliari
SS 554, bivio per Sestu, 09042 Monserrato, Cagliari (Italy)
E-mail: giuseppe.sforazzini@unica.it

Supporting information for this article is available on the WWW under https://doi.org/10.1002/chem.202202698

Thus, molecular designs that exploit nonchemical stimuli, such as light, are the best candidates to create responsive organic semiconductors for the development of new optoelectronic technologies.[34,35] To date, examples of light-responsive molecular actuators conceived to tune the effective conjugation length of linear π-systems have been mainly based on two paradigms: the cleavage-formation of π-bonds,[36–39] and the torsion planarization of p-orbitals' nodal plane.[40–42] The first class of compounds, for example, diarylethenes, is generally incorporated as monomeric unit into π-conjugated backbone of oligomers and polymers, the second, instead, is usually placed as a side functionality along linear π-conjugated systems. Recently Peters and Tovar have shown that diarylethenes can also be engineered as a side functionality to tune the planarization of the π-system.[43] Despite the inherent differences in the molecular design of two aforementioned categories of compounds, their functionality suffers from some limitations (Figure 1).

Molecular architectures that rely on the cleavage-formation of π-bonds often reduce their operation reversibility efficiency as their π-conjugation extension increases.[44–47] On the other hand, the design of the molecular actuators that modulate the

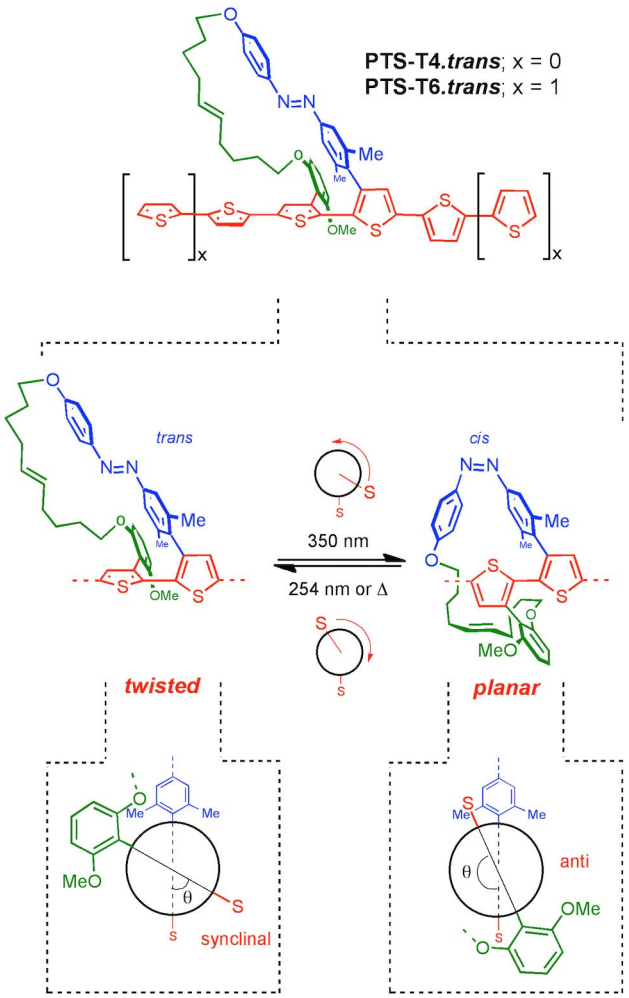

Figure 1. Schematics of molecules studied in this work.

π-bond geometry of a conjugated system are commonly restricted to the possibility to assume only semiplanar conformations (e.g., *syn* and *anti*) that are similar in their electronic structures.[40–42]

In our previous work, we reported a novel design for these molecular actuators. We introduced a light-driven molecular switch (azobenzene) in an orthogonal fashion to a linear π-conjugated system (bithiophene), thus to suppress the detrimental reduction of switchability due to extension of the π-conjugation. At the same time, the thoughtful design of a side-chain linker, connecting the azobenzene to bithiophene unit, achieved highly twisted π-bond geometry along the bithiophenic segment. The described macrocyclic architecture, which consists of an azobenzene, a bithiophene and a linker, is referred to as photochromic torsional switch (PTS) unit.[48] In this work, we demonstrate that PTS-based π-conjugated derivatives can indeed reversibly tune their effective conjugation length by using light as an external stimulus. Herein, we report the synthesis of two novel PTS thiophene-based light-responsive π-conjugated compounds (quaterthiophene and sexithiophene), and we highlight the relationship between their structures and optical properties by spectroscopic and computational investigations. Finally, we test their ability to modulate the charge percolation in optoelectronic devices by employing them as active layer into organic field effect transistors (OFETs).

Results and Discussion

Synthesis and XRD molecular characterization

The synthesis of the PTS-based oligothiophenes was achieved as summarized in Figure 2a. First the PTS unit (**PTS-T2**) was prepared through a convergent route affording the sole *trans*-twisted conformer.[48] The latter was then functionalized in both 2-positions of thiophene rings using LDA followed by I_2 or trimethyltin chloride, to achieve the corresponding 2,2′-halides (**1**) and 2,2′-stannanes (**2**) derivatives. The PTS-based quaterthiophene (**PTS-T4.*trans***) and sexithiophene (**PTS-T6.*trans***) were synthesized by Suzuki and Stille coupling of PTS bithiophene 2,2′-halides and 2,2′-stannanes, respectively, with monofunctionalized thiophene and bithiophene bearing complementary functionalities (for details about the synthesis, see the Supporting Information). Single crystals of **PTS-T2**, **PTS-T4**, and **PTS-T6** molecules were grown from tetrahydrofuran solution using vapor diffusion of hexane. The X-ray crystallographic analysis of **PTS-T2**, **PTS-T4**, and **PTS-T6** revealed atropisomers packed in centrosymmetric $P2_1/c$, $P\bar{1}$ and $C2/c$ unit cells, respectively (for more details on the cell unit and packing see the Supporting Information). The dihedral angles (θ) between the two PTS thiophenic subunits were found to be $\theta = 60°$ for the pristine PTS unit **PTS-T2**, $\theta = 57°$ and $\theta = 58°$ for **PTS-T4**, and **PTS-T6**, respectively (Figure 2b). The oligothiophene backbone assumes a twisted geometry at the center, decoupling the two halves (subunits) that are planar. Analysis of the packing shows that in the case of **PTS-T2**, which lacks lateral aromatic extension, no close contacts between thiophene rings were observed. In **PTS-**

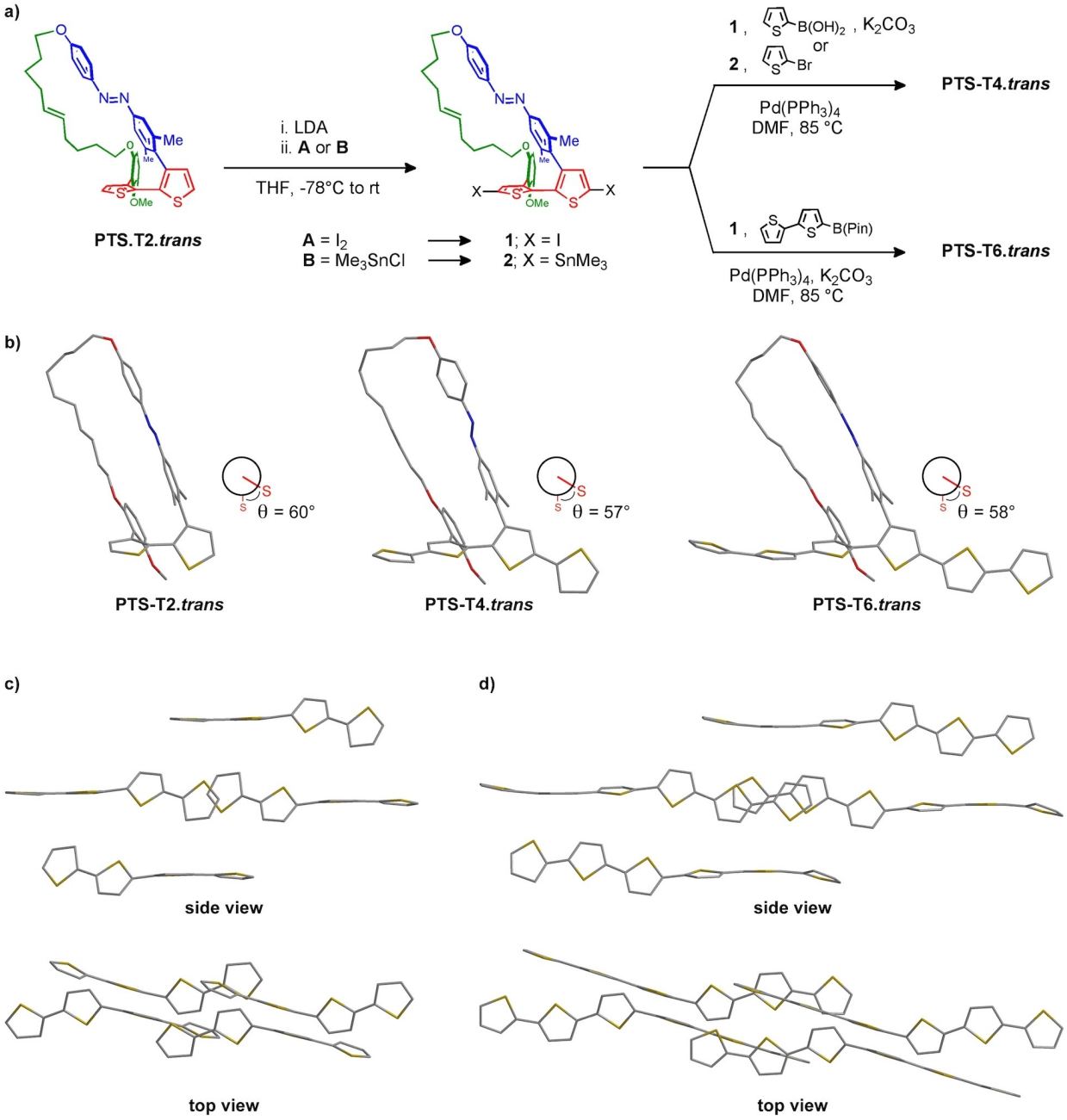

Figure 2. a) Synthetic pathway for **PTS-T4** and **PTS-T6** from the PTS unit **PTS-T2**. b) X-ray single-crystal structures of **PTS-T2.*trans***, **PTS-T4.*trans*** and **PTS-T6.*trans***. Selected parts of the solid-state structures of c) **PTS-T4.*trans*** and d) **PTS-T6.*trans*** showing the arrangement of thiophene units.

T4, the terminal thiophene rings of two neighboring molecules adopt a slipped π–π staking arrangement, also exhibiting a S···S interaction ($d_{S\text{-}S} = 3.6$ Å, Figure 2c), often observed in solid-state structures of sulfur containing compounds.[49] The stacked dimer is further surrounded from both sides by nearly orthogonal thiophene rings. The **PTS-T6** displayed similar packing pattern featuring π–π stacked dimer surrounded by thiophene rings (Figure 2d).

In contrast to **PTS-T4**, the thiophene-rich regions in **PTS-T6** involve stacking and orthogonal T arrangement (edge-to-face) between extended dithiophene regions rather than single thiophene rings as in **PTS-T4**, thus suggesting its possibly better charge conducting properties.[50] Moreover, the stacking of thiophene rings in **PTS-T6** is realized in parallel fashion with respect to sulfur atoms whereas in **PTS-T4** antiparallel arrangement is observed (for details see the Supporting Information).

Spectroscopic characterization and quantum chemical modeling

The absorption spectra of the *trans* PTS derivatives, **PTS-T4.*trans*** and **PTS-T6.*trans***, exhibit a main broad band at 358 nm and 379 nm, respectively (Figure 3a). The signatures of these two spectra differ significantly from that of the pristine **PTS-T2.*trans*** where the contributions of the two constituting components, the bithiophene and the azobenzene, are well distinguishable with a band at 284 nm for the former and a peak centered around 363 nm for the latter.[48] The observed broad band in the absorption spectrum of **PTS-T4.*trans*** and **PTS-T6.*trans*** can be attributed to a spectral overlap of the electronic transition of the azobenzene and that of the oligothiophene backbone. As the azobenzene is disposed orthogonally to the thiophenic π-system, it is not expected to undergo any significant change in its absorption spectrum with the elongation of the thiophene-based chain. However, the gradual π-extension from the bithiophene to the sexithiophene lowers the excitation energy of the thiophenic backbone resulting in a spectral shift towards longer wavelengths. The anticipated bathochromic shift might cause a superimposition with the absorption band of the azobenzene ($\lambda_{max} = \sim 363$ nm). Considering that the PTS motif twists the oligothiophene backbone in its middle, we could expect that the spectral contribution of the twisted quaterthiophene in **PTS-T4.*trans*** is red-shifted with respect to that of its half segment (bithiophene, $\lambda_{max} = \sim 303$ nm) and blue-shifted with respect to its extended form (quaterthiophene, $\lambda_{max} = \sim 392$ nm; Figure 3c).[51] Similarly, the twisted backbone of **PTS-T6.*trans*** can be expected to have its absorption band between that of the terthiophene ($\lambda_{max} = \sim 354$ nm) and that of an extended sexithiophene ($\lambda_{max} = \sim 436$ nm; Figure 3c).[51] To get insights into the excited states of **PTS-T*n*.*trans*** and better characterize the band overlap in the UV-Vis spectra, we performed excited-state quantum-chemical calculations on lowest-energy conformers, as obtained by a combined tight-binding DFT-based approach and further full DFT refinements (see the Supporting Information and computational methods).[52–54] According to time dependent density functional theory (TDDFT),[55] the observed absorption band of both **PTS-T4.*trans*** (358 nm) and **PTS-T6.*trans*** (379 nm) involves two competing electronic transitions: one, here called $S_0 \rightarrow S^*_{thio}$, that is localized on the oligothiophene chain, and another one, named $S_0 \rightarrow S^*_{azo}$, that is localized on the azobenzene unit. For **PTS-T4.*trans*** the $S_0 \rightarrow S^*_{thio}$ is ascribed to the $S_0 \rightarrow S_3$ one-electron transition that is mainly described as the highest occupied molecular orbital (HOMO) to the lowest unoccupied molecular orbital (LUMO) + 1 transition, both orbitals localized on the thiophenic backbone. The $S_0 \rightarrow S^*_{azo}$ is associated to the $S_0 \rightarrow S_2$ transition prevalently involving the HOMO-1 to LUMO, the latter mainly localized on azobenzene (Section 5 in the Supporting Information). TDDFT calculations show that the two transitions are 13 nm apart one from the other, so confirming the superimposition between the absorption bands of the quaterthiophene and the azobenzene. In the case of **PTS-T6.*trans***, the $S_0 \rightarrow S^*_{thio}$ is characterized by the $S_0 \rightarrow S_2$ one-electron transition prevalently described as HOMO→LUMO + 1 of the backbone, while the $S_0 \rightarrow S^*_{azo}$ involves multiple one-electron transitions with the HOMO-1→LUMO as dominant. These two competing transitions lie in close proximity within 17 nm, so confirming a spectral overlap between the absorption bands of sexithiophene and that of azobenzene (Section 5 in the Supporting Information). In addition, TDDFT calculations show that by extending the thiophenic chain, from **PTS-T4.*trans*** to **PTS-T6.*trans***, the $S_0 \rightarrow S^*_{thio}$ transition undergoes a bathochromic shift of ~30 nm, in accordance with the increased π-electron conjugation of the oligothiophene unit (Section 5.2 in the Supporting Information). Upon irradiation at 350 nm approximately 49% of **PTS-T4.*trans*** and 57% of **PTS-T6.*trans*** are converted to their *cis*-planar isomers.

The absorption spectrum of the former exhibits one main broad band centered at ~366 nm (Figure 3b), which is blue-shifted of about 26 nm with respect to the λ_{max} of a regular quaterthiophene, (Figure 3c).[51] The observed hypsochromic shift can be ascribed to the parasite spectral contributions

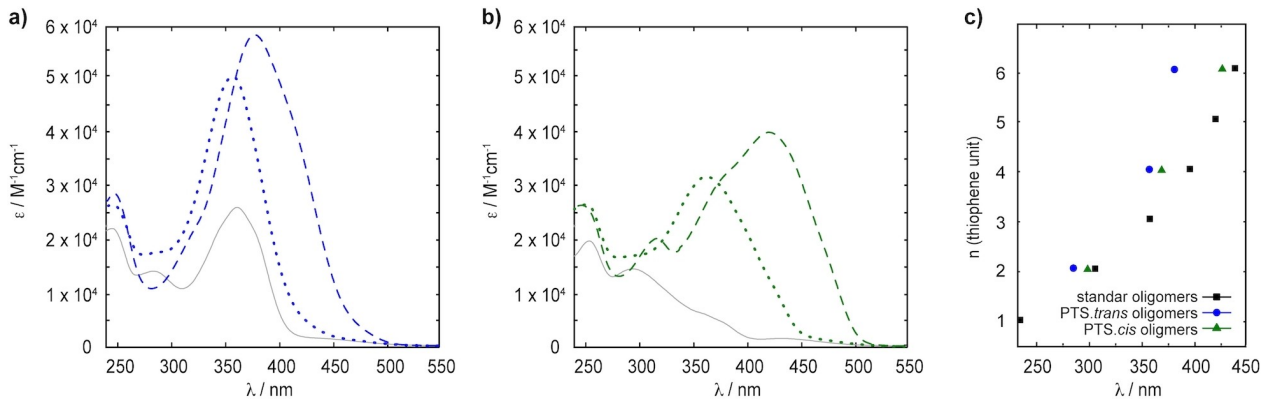

Figure 3. a) Absorption spectra of **PTS-T2.*trans*** (solid gray line), **PTS-T4.*trans*** (dotted blue line), and **PTS-T6.*trans*** (dashed blue line) in THF. b) Absorption spectra of **PTS-T2.*cis*** (solid gray line), **PTS-T4.*cis*** (dotted green line), and **PTS-T6.*cis*** (dashed green line) in THF. c) Plot of the absorption λ_{max} of **PTS-T2**, **PTS-T4**, and **PTS-T6** in their twisted-*trans* (blue) and planar-*cis* (green) forms, and selected pristine oligothiophenes (di-, tert-,quater-, penta-, sexithiophenes, black) reported in literature.[51]

involving the twisted-quaterthiophene and the azobenzene, in its *trans* and *cis* forms. Such a scenario is plausible as **PTS-T4** reaches a photostationary state (PSS) once is irradiated at 350 nm. In the case of **PTS-T6.*cis***, the absorption spectrum shows three distinguishable bands: a main one at 424 nm, a shoulder at 387 nm, and one at 319 nm (Figure 3b). The first and the third bands are significantly close to the wavelengths commonly reported for a pristine sexithiophene ($\lambda_{max}=436$ nm and $\lambda=314$ nm).[52] This finding suggests that the planar arrangement assumed by the oligothiophene backbone upon photo-isomerization of the azobenzene to its *cis* form is reasonably close to the structure of the pristine sexithiophene. However, the band at 387 nm indicates the presence of competitive absorbing species that generate a PSS for **PTS-T6**.

In order to understand the correlation between the absorption spectra and the structural changes induced by the azobenzene to the oligothiophene backbone, we first computed the **PTS-T4.*cis*** and **PTS-T6.*cis*** lowest-energy conformers, by performing as for the case of **PTS-T*n*.*trans*** a multi-level conformational screening followed by TDDFT calculations. It has to be noted that the computational investigations were essential to determine the equilibrium molecular structures of **PTS-T4.*cis*** and **PTS-T6.*cis***, as these compounds spontaneously return to their initial *trans*-twisted conformation within a day, so hampering the possibility to grow crystals. DFT calculations of **PTS-T4.*cis*** and **PTS-T6.*cis*** show that when the azobenzene is in its *cis* form the oligothiophene backbone assumes a more planar conformation with $\theta=152.4°$ and 152.3°, respectively (Figure 4). The latter values are in good agreement within the range of dihedral angles reported in literature for unsubstituted bi-, quater-, and sexithiophenes in their *anti*-conformation ($\theta=$ 146–152°).[56,57] According to TDDFT calculations, performed for the most stable conformers, the main bands in the computed absorption spectra of **PTS-T4.*cis*** and **PTS-T6.*cis*** can be assigned to the sole $S_0\rightarrow S^*_{thio}$ transition, deriving from the $S_0\rightarrow S_2$ excitation mainly involving HOMO and LUMO which are prevalently localized on oligothiophene chain (anti conformation; see Section 5 in the Supporting Information). By the analysis of DFT and TDDFT calculations, we can deduce that when the azobenzene isomerizes from *trans* to *cis*, it reduces the dihedral angle of the central bithiophene and at the same time assists the planarization of the whole oligothiophene backbone. The adoption of these planar conformations results in a remarkable optical response from the oligothiophene moiety, with a bathochromic shift for the $S_0\rightarrow S^*_{thio}$ transition of 42 nm for **PTS-T4** and of 37 nm for **PTS-T6**. As anticipated, the main absorption bands measured for **PTS-T4.*cis*** and **PTS-T6.*cis*** still have some contributions from the electronic transitions of the unconverted **PTS-T4.*trans*** and **PTS-T6.*trans*** (both $S_0\rightarrow S^*_{thio}$ and $S_0\rightarrow S^*_{azo}$). Thus, while for **PTS-T6** the spectral shift from the *trans*-twisted to the *cis*-planar form is clearly visible, for **PTS-T4** it is less pronounced.

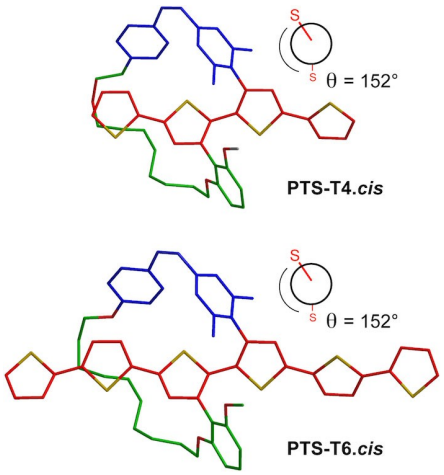

Figure 4. DFT (ωB97X-D/6-311+G*)-optimized geometries of **PTS-T4.*cis*** and **PTS-T6.*cis***.

Photoswitchability and thermal relaxation

PTS-based oligothiophene **PTS-T4** and **PTS-T6** can reversibly switch between their *trans*-twisted and *cis*-planar forms. After their *trans*-to-*cis* isomerization **PTS-T4** and **PTS-T6** can recover about ~83 and ~79% of the initial absorption intensity by irradiating at 254 nm (Figure 5a, b).[58] The wavelength was selected as an alternative excitation to the usual n–π^* transition for the *cis*-to-*trans* isomerization which, in the alkoxyazobenzenes, is usually ascribed to an absorption band around ~440 nm.[59,60] The latter is inaccessible in our systems due to the competitive absorption of the oligothiophene backbone. Moreover, the structural constrain of azobenzene in the PTS derivatives leads to a similar oscillator strengths for the n–π^* transition of the *trans* and *cis* conformers, so making excitation at this absorption band moderately effective for *cis*-to-*trans* isomerization. Excitation around 250 nm promote the ϕ–ϕ^* transition of azobenzenes which exhibits no influence from the structural constraint of the PTS architecture.[48,60]

In contrast to what we previously published for the *cis* form of the parent PTS unit (**PTS-T2**) in its *cis* form, **PTS-T4.*cis*** and **PTS-T6.*cis*** return spontaneously to their *trans* forms by thermal relaxation within 1–1.5 days. In addition, the velocity of this process increases directly with the extension of the thiophene-based backbone π-conjugation. **PTS-T4** and **PTS-T6** recover about ~95% of the initial absorption intensity within 36 and 24 h, respectively (Figure 5c, d). These enhanced thermal relaxations are unexpected as the structural constraint of the PTS unit is retained in both **PTS-T4** and **PTS-T6**, and as the extension at of π-conjugation take place along the oligothiophenes backbone and not on the azobenzene.

The analysis of the computed frontier molecular orbitals of PTS derivatives shows that the lengthening of the thiophenic backbone π-conjugation (from T4 to T6) increases the overlap and the "cross-conjugation" between the localized molecular orbitals of the azobenzene unit and those of the thiophenic chain (Figure S4). The electronic coupling between these pseudo-orthogonal frontier orbitals induces a polarization along the azobenzene unit with an electron-rich area onto the phenolic segment, and a relatively electron-poor part around

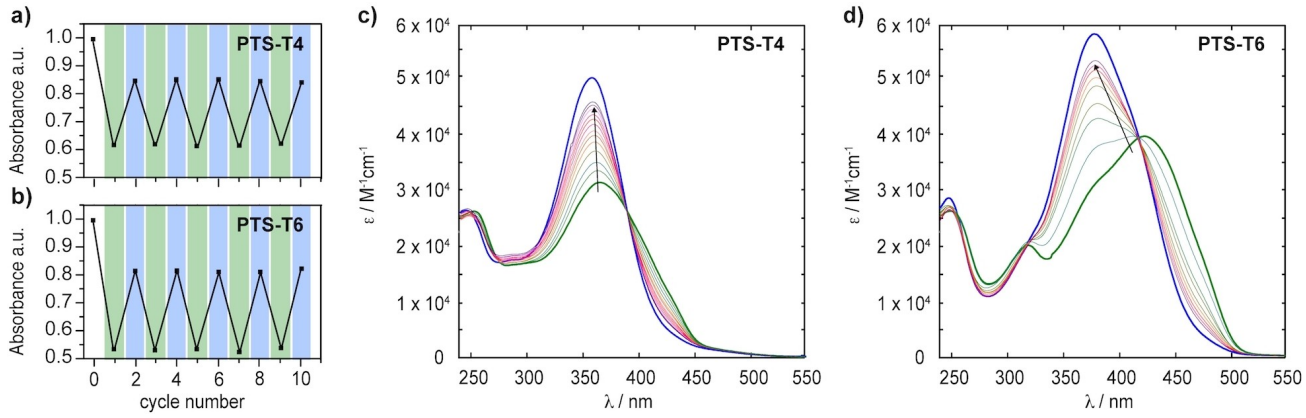

Figure 5. Photoswitching of a) **PTS-T4** and b) **PTS-T6**. Thermal relaxation from *cis*-to-*trans* of c) **PTS-T4** and d) **PTS-T6** in THF at 25 °C; the arrows show the spectral change over time.

dimethylbenzene. This effect is particularly evident for the **PTS-T6.*trans*** species, characterized by a strong electronic coupling between the localized orbitals of the azobenzene units and those of the sexithiophene chain, leading to a hybridized orbital picture (Figure S4). Such a scenario resemble the electronic configuration of push–pull azobenzene that are known to have extremely short *cis* isomer lifetime.[61] Thus, by extending the backbone π-conjugation of PTS-based architectures it is possible to tune the switching properties of the azobenzene moiety. To the best of our knowledge, the enhancement of the azobenzene *cis*-to-*trans* thermal relaxation with the increasing conjugation of an orthogonally attached π-system has never reported before.

Charge transport

To investigate if the conformational changes induced by the azobenzene to the conjugated backbone affects the charge transport properties of the PTS derivatives, we fabricated bottom gate bottom contact transistors containing PTS-based oligothiophenes as the active semiconducting layer (for details, see Section 6 in the Supporting Information). Thin-films of **PTS-T4** and **PTS-T6** were solution processed by spin coating in its *trans*-twisted form and its hole mobility (μ_h) was measured. Transistors containing **PTS-T4.*trans*** did not exhibit any charge transport, while **PTS-T6.*trans*** displayed a μ_h of $4\times10^{-6}\,cm^{-2}V^{-1}s^{-1}$ (Figure 6). The latter was then irradiated with UV light at a wavelength of 350 nm for 10 min and its transistor performance measured. After irradiation, the charge mobility decreased to $\mu = 5\times10^{-7}\,cm^{-2}V^{-1}s^{-1}$, but recovered to $\mu = \sim3.5\times10^{-5}\,cm^{-2}V^{-1}s^{-1}$ after storing in the dark for 24 h under nitrogen in a glovebox (Section 6 in the Supporting Information). The observed reduction of charge transport can be ascribed to the change in molecular packing induced by the photo-activated *trans*-to-*cis* isomerization of the PTS unit as discussed above. Meanwhile the recovery of the charge transport is likely due to the azobenzene undergoing a *cis*-to-*trans* isomerization over time. However, the enhanced charge mobility upon recovering the initial *trans*-twisted conformation might suggest that PTS-based molecules have assumed a more efficient packing for charge percolation after a full cycle compared to the prepared film. This promising preliminary result governs a further in-depth investigation that is currently on-going and will be reported elsewhere.

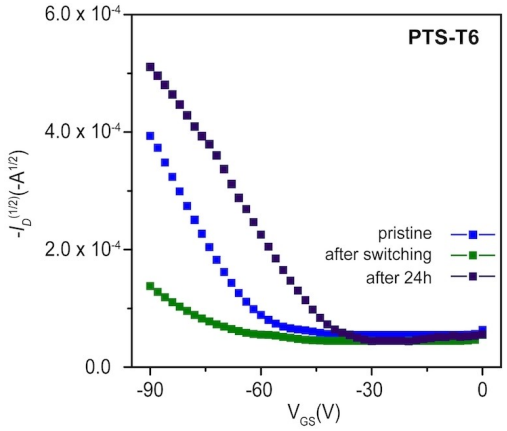

Figure 6. Transfer curves of **PTS-T6** in a bottom gate bottom contact field-effect transistor.

Conclusion

A novel class of light-responsive oligothiophenes has been synthetized by using the PTS architecture as a molecular-actuator. PTS-based quaterthiophene and sexithiophene reversibly tune their optical properties in response to light, and exhibit an enhanced thermal relaxation proportional to their backbone π-conjugation extension. Moreover, a preliminary investigation on their use as an active layer in OFETs suggests that the proposed PTS-based derivatives can be successfully used for the development of a new generation of light-responsive optoelectronic devices.

Experimental Section

General remarks: Air- or water-sensitive compounds were manipulated by using standard high vacuum techniques. DCM, acetone, petroleum ether, heptanes, EtOAc and toluene were purchased from Reactolab SA and distilled under reduced pressure before use. All other reagents were used as supplied. THF (99.99%), and diisopropylamine were purchased from Fischer Scientific. K_2CO_3 (99+%, anhydrous), *n*-butyllithium (1.6 M in hexane) and DMF (99.8%, extra dry, acroseal) were purchased from Acros organics. Iodine, 2-bromothiophene, and 2-([2,2′-bithiophen]-5-yl)-4,4,5,5-tetramethyl-1,3,2-dioxaborolane were purchased from TCI. Dioxane (>99.5%), Pd(PPh3)4, trimethyltin chloride, and Grubbs catalyst 2nd generation were purchased from Sigma-Aldrich. Analytical thin-layer chromatography (TLC) was carried out on Merck aluminium backed silica gel 60 GF254 plates. Column chromatography was carried out on silica gel 60 GF254 (particle size 40–63 μm, Merck) using positive air pressure. NMR spectra were recorded at ambient probe temperature using the following Fourier transform instruments: Bruker Avance III 400 MHz (9.0 T) equipped with BBFO probe, and Bruker Avance III 600 MHz (14.1 T) equipped with TCI CryoProbe. Chemical shifts (δH and δC) are reported in parts per million (ppm) relative to the residual solvent peak. Coupling constants (*J*) are reported in Hertz. Accurate mass determinations using ESI (HR ESI-MS) were performed on a Xevo G2-S QTOF mass spectrometer. UV-Vis spectra were recorded on a JASCO V-670 spectrophotometer and the absorption wavelengths (λ) are reported in nm (extinction coefficient ε in M−1 cm−1). Photoisomerizations were carried using a Camag UV lamp TL 900/U.

Synthesis

PTS-T2.*trans*: This compound was synthesized according to reported procedures.[48]

Compound 1: *n*-Butyllithium in hexane (0.41 mL, 0.641 mmol) was added slowly at −78 °C to a solution of diisopropylamine (0.099 mL, 0.705 mmol) in dry THF (0.8 mL) under argon. The mixture was allowed to reach 0 °C and stirred for 10 min. at this temperature. To a solution of compound **PTS-T2.*trans*** (104 mg, 0.160 mmol) in dry THF (1.3 mL) at −78 °C was slowly added a freshly prepared above solution of LDA. The mixture was stirred for 3 h and then a solution of iodine (244 mg, 0.962 mmol) in dry THF (0.4 mL) was added to the reaction mixture at −78 °C. The reaction was stirred for 24 h allowing slowly reach the room temperature. Reaction was quenched with sat. NH_4Cl solution, extracted with ethyl acetate, washed with brine, dried with $MgSO_4$ and the solvent was removed under reduced pressure. The product was purified by column chromatography on silica gel (eluent PE/DCM 1:1) to give a brown oil 87 mg (60%) of **1**. ^{1}H NMR (400 MHz, [D_8]THF): δ = 7.90 (d, *J* = 8.8 Hz, 2H), 7.40 (s, 1H), 7.20 (s, 1H), 7.13 (t, *J* = 8.3 Hz, 1H), 7.07 (d, *J* = 8.9 Hz, 2H), 7.03 (s, 1H), 6.83 (s, 1H), 6.39 (d, *J* = 8.3 Hz, 1H), 6.29 (d, *J* = 8.3 Hz, 1H), 4.93–4.88 (m, 2H), 4.36–4.30 (m, 2H), 3.50 (s, 3H), 3.33–3.26 (m, 1H), 3.15–3.07 (m, 1H), 1.97 (s, 3H), 1.93–1.88 (m, 2H), 1.63–1.55 (m, 2H), 1.54–1.46 (m, 4H), 1.38 (s, 3H), 1.24–1.18 (m, 1H), 1.12–1.04 (m, 1H), 0.76–0.70 (m, 1H), 0.65–0.58 (m, 1H); ^{13}C NMR (101 MHz, [D_8]THF): δ = 160.64, 158.62, 157.99, 152.00, 147.79, 142.26, 140.96, 139.82, 139.37, 139.12, 138.01, 137.29, 136.67, 136.16, 131.50, 130.05, 128.88, 124.91, 122.38, 121.19, 117.99, 112.10, 104.32, 103.71, 74.92, 72.76, 68.34, 67.84, 55.16, 33.31, 31.47, 29.47, 26.01, 25.60, 23.87, 20.99, 20.18; HRMS (ESI, positive mode) *m/z* calcd for $C_{39}H_{39}I_2N_2O_3S_2$ $[M+H]^+$: 901.0486; found: 901.0474.

Compound 2: *n*-Butyllithium in hexane (0.17 mL, 0.421 mmol) was added slowly at −78 °C to a solution of diisopropylamine (0.065 mL, 0.463 mmol) in dry THF (0.5 mL) under argon. The mixture was allowed to reach 0 °C and stirred for 10 min. To a solution of **PTS-T2.*trans*** (68 mg, 0.105 mmol) in dry THF (0.9 mL) at −78 °C was slowly added a freshly prepared above solution of LDA. The mixture was stirred for 3 h and then a solution of trimethyltin chloride (126 mg, 0.631 mmol) in dry THF (0.3 mL) was added to a reaction mixture at −78 °C. The reaction was stirred allowing for 24 h allowing slowly reach room temperature. Reaction was diluted with ethyl acetate, washed with water, dried with $MgSO_4$ and solvent removed under reduced pressure. The product 2 (93.8 mg, 98%) was used without further purification. ^{1}H NMR (400 MHz, [D_8]THF): δ = 7.89 (d, *J* = 8.8 Hz, 2H), 7.34 (s, 1H), 7.18 (s, 1H), 7.08 (t, *J* = 8.3 Hz, 1H), 7.06 (d, *J* = 8.9 Hz, 2H), 6.88 (s, 1H), 6.76 (s, 1H), 6.33 (d, *J* = 8.3, 1H), 6.25 (d, *J* = 8.3, 1H), 4.90 (t, *J* = 3.1 Hz, 2H), 4.34–4.30 (m, 2H), 3.38 (s, 3H), 3.32–3.25 (m, 1H), 3.12–3.04 (m, 1H), 1.94–1.89 (m, 2H), 1.87 (s, 3H), 1.63–1.55 (m, 2H), 1.53–1.46 (m, 4H), 1.43 (s, 3H), 1.21–1.14 (m, 1H), 1.13–1.05 (m, 1H), 0.78–0.70 (m, 1H), 0.67–0.61 (m, 1H), 0.46 (s, 1H), 0.39 (s, 7H), 0.30 (s, 8H), 0.23 (t, *J* = 5.0 Hz, 2H); ^{13}C NMR (101 MHz, [D_8]THF): δ = 157.77, 155.96, 155.41, 148.93, 145.23, 138.45, 138.22, 136.53, 136.52, 136.24, 135.56, 135.48, 135.28, 133.04, 131.80, 128.85, 126.33, 126.28, 122.13, 119.94, 118.06, 115.34, 111.59, 109.97, 101.55, 101.15, 65.43, 65.20, 52.32, 30.68, 28.86, 26.85, 23.46, 23.03, 21.29, 18.49, 17.87, −11.26, −11.29; HRMS (ESI, positive mode) *m/z* calcd for $C_{45}H_{57}N_2O_3S_2Sn_2$ $[M+H]^+$: 975,1843; found: 975.1860.

PTS-T4.*trans*: (Method A) A mixture of compound **1** (30 mg, 0.033 mmol), 2-thiopheneboronic acid (21 mg, 0.167 mmol), Pd-$(PPh_3)_4$ (7.6 mg, 0.007 mmol), and K_2CO_3 (23 mg, 0.166 mmol) were dissolved in DMF (1 mL) under argon. The mixture was heated to 85 °C with stirring18 h. The reaction mixture was allowed to reach room temperature and then diluted with ethyl acetate, washed with brine, dried with $MgSO_4$ and evaporated to dryness. The product was purified by column chromatography on silica gel (eluent PE/DCM 1:1) and short silica pad afterwards (eluent PE:EA 9.5:0.5) to give 16.8 mg (62%) of **PTS-T4.*trans*** as an orange solid. (Method B) A mixture of 2 (79 mg, 0.088 mmol), 2-bromothiophene (42 μL; 0.437 mmol) and $Pd(PPh_3)_4$ (20 mg, 0.018 mmol) was dissolved in DMF (2.6 mL) under argon. The mixture was heated to 85 °C and stirred for 15 h. The reaction mixture was allowed to reach room temperature and then diluted with ethyl acetate, washed with brine, dried with MgSO4 and evaporated under reduced pressure. The product was purified by column chromatography on silica gel (eluent PE/DCM 1:1) to give 29 mg (41%) of **PTS-T4.*trans*** as an orange solid. ^{1}H NMR (400 MHz, [D_8]THF): δ = 7.91 (d, *J* = 8.8 Hz, 2H), 7.42 (s, 1H), 7.34 (d, *J* = 5.1 Hz, 1H), 7.30 (d, *J* = 3.6 Hz, 1H), 7.26 (d, *J* = 4.9 Hz, 1H), 7.23 (s, 1H), 7.16 (d, *J* = 2.4 Hz, 1H), 7.14 (t, *J* = 8.3 Hz, 1H), 7.07 (d, *J* = 9.0 Hz, 2H), 7.04 (dd, *J* = 5.5, 4.3 Hz, 1H), 7.02 (s, 1H), 6.98 (dd, *J* = 5.0, 3.6 Hz, 1H), 6.85 (s, 1H), 6.41 (d, *J* = 8.3 Hz, 1H), 6.31 (d, *J* = 8.3 Hz, 1H), 4.93–4.88 (m, 2H), 4.38–4.29 (m, 2H), 3.53 (s, 3H), 3.38–3.29 (m, 1H), 3.19–3.09 (m, 1H), 2.05 (s, 3H), 1.94–1.87 (s, 2H), 1.63–1.55 (m, 2H), 1.52–1.44 (m, 7H), 1.30–1.20 (m, 1H), 1.17–1.08 (m, 1H), 0.80–0.70 (m, 1H), 0.69–0.57 (m, 1H); ^{13}C NMR (101 MHz, THF): 160.56, 158.60, 158.19, 151.90, 147.83, 139.89, 139.27, 138.18, 138.08, 137.91, 137.89, 137.77, 136.11, 135.04, 133.02, 131.50, 131.28, 129.76, 129.18, 128.88, 128.48, 128.32, 126.62, 125.24, 124.87, 124.77, 124.29, 123.76, 122.45, 121.19, 117.99, 113.40, 104.32, 103.82, 68.29, 67.83, 55.28, 33.30, 31.49, 29.55, 26.05, 25.60, 23.87, 21.13, 20.38. HRMS (ESI, positive mode) *m/z* calcd for C47H45N2O3S4 $[M+H]^+$: 813.2308; found: 813.2307; $\varepsilon = 5.05\times10^4$ Lmol^{-1}cm^{-1} (λ_{max} = 358 nm).

PTS-T6.*trans*: A mixture of **1** (49.2 mg, 0.055 mmol), 2-([2,2′-Bithiophen]-5-yl)-4,4,5,5-tetramethyl-1,3,2-dioxaborolane (79.9 mg, 0.273 mmol), Pd(PPh3)4 (12.6 mg, 0.011 mmol), and K_2CO_3 (37.7 mg, 0.273 mmol) were dissolved in DMF (1 mL) under argon. The mixture was heated to 85 °C and stirred for 2 h. The reaction mixture was allowed to reach room temperature and then diluted with dichloromethane, washed with brine, dried with MgSO4 and

evaporated under reduced pressure. The product was purified by column chromatography on silica gel (eluent PE/DCM 1:1) to afford 35 mg (66%) of **PTS-T6.*trans*** as an orange solid. ^{1}H NMR (400 MHz, THF): $\delta = 7.91$ (d, $J = 8.8$ Hz, 2H), 7.43 (s, 1H), 7.34 (d, $J = 5.0$ Hz, 1H), 7.91 (d, $J = 8.8$ Hz, 1H), 7.25 (d, $J = 3.6$ Hz, 2H), 7.24 (s, 1H), 7.19 (t, $J = 3.3$ Hz, 2H), 7.16 (t, $J = 8.3$ Hz, 1H), 7.11 (q, $J = 3.9$ Hz, 2H), 7.07 (d, $J = 8.9$ Hz, 2H), 7.06 (s, 1H), 7.03 (dd, $J = 5.0$, 3.7 Hz, 1H), 6.99 (dd, $J = 5.0$, 3.7 Hz, 1H), 6.88 (s, 1H), 6.42 (d, $J = 8.3$ Hz, 1H), 6.32 (d, $J = 8.4$ Hz, 1H), 4.94–4.88 (m, 2H), 4.37–4.28 (m, 2H), 3.54 (s, 3H), 3.38–3.30 (m, 1H), 3.21–3.09 (m, 1H), 2.06 (s, 3H), 1.95–1.86 (m, 2H), 1.65–1.55 (m, 2H), 1.55–1.44 (m, 7H), 1.33–1.21 (m, 1H), 1.20–1.07 (m, 1H), 0.81–0.71 (m, 1H), 0.69–0.59 (m, 1H); ^{13}C NMR (101 MHz, THF): 160.59, 158.60, 158.18, 151.95, 147.84, 140.12, 139.27, 138.18, 137.76, 137.69, 137.61, 137.38, 137.13, 136.84, 136.68, 136.60, 135.78, 135.29, 133.25, 131.53, 131.51, 129.85, 129.37, 128.88, 128.56, 128.47, 126.85, 125.42, 125.23, 125.07, 125.03, 124.93, 124.90, 124.58, 124.44, 124.30, 122.48, 121.26, 118.00, 113.27, 104.36, 103.85, 68.35, 67.84, 55.30, 33.30, 31.49, 29.56, 26.07, 25.60, 23.87, 21.13, 20.41; HRMS (ESI, positive mode) *m/z* calcd for $C_{55}H_{49}N_2O_3S_6$ $[M+H]^+$: 977.2062; found: 977.2067; $\varepsilon = 5.85 \times 10^4$ $Lmol^{-1}cm^{-1}$ ($\lambda_{max} = 379$ nm).

Deposition Numbers COD 3000407 (for **PTS-T2**.*trans*), COD 3000408 (for **PTS-T4**.*trans*) and COD 3000409 (for **PTS-T6**.*trans*) contain the supplementary crystallographic data for this paper. These data are provided free of charge by the Crystallography Open Database (http://www.crystallography.net/cod/).

Acknowledgements

G. S. would like to thank Prof. Holger Frauenrath for his helpful discussions, the Swiss National Science Foundation (SNF grant no. PZ00P2_148050), and the Fondazione di Sardegna (annualità 2020, FdS grant no. F75F21001250007) for their financial support. E. O. would like to thank the Research Council of Lithuania (grant no. S-MIP-22-69) for the financial support. Open Access funding provided by Università degli Studi di Cagliari within the CRUI-CARE Agreement.

Conflict of Interest

The authors declare no conflict of interest.

Data Availability Statement

The data that support the findings of this study are available from the corresponding author upon reasonable request.

Keywords: azobenzene · conjugation tuning · molecular actuators · oligothiophenes · twisted π-system

[1] A. Salehi, X. Fu, D. Shin, F. So, *Adv. Funct. Mater.* **2019**, *29*, 1808803.
[2] L. Cao, Z. Zhu, K. Klimes, J. Li, *Adv. Mater.* **2021**, *33*, 2101423.
[3] J. Bauri, R. B. Choudhary, G. Mandal, *J. Mater. Sci.* **2021**, *56*, 18837–18866.
[4] M. J. Frampton, G. Sforazzini, S. Brovelli, G. Latini, E. Townsend, C. C. Williams, A. Charas, L. Zalewski, N. S. Kaka, M. Sirish, L. J. Parrott, J. S. Wilson, F. Cacialli, H. L. Anderson, *Adv. Funct. Mater.* **2008**, *18*, 3367–3376.
[5] S. Brovelli, G. Sforazzini, M. Serri, G. Winroth, K. Suzuki, F. Meinardi, H. L. Anderson, F. Cacialli, *Adv. Funct. Mater.* **2012**, *22*, 4284–4291.
[6] C. Lee, S. Lee, G. Kim, W. Lee, B. J. Kim, *Chem. Rev.* **2019**, *119*, 8028–8086.
[7] S. Shoaee, A. L. Sanna, G. Sforazzini, *Molecules* **2021**, *26*, 7439.
[8] R. Zhou, Z. Jiang, C. Yang, J. Yu, J. Feng, M. A. Adil, *Nat. Commun.* **2019**, *10*, 5393.
[9] Y. Cui, Y. Xu, H. Yao, P. Bi, L. Hong, J. Zhang, Y. Zu, T. Zhang, J. Qin, J. Ren, Z. Chen, C. He, X. Hao, Z. Wei, J. Hou, *Adv. Mater.* **2021**, *33*, 2102420.
[10] A. Rahmanudin, R. Marcial-Hernandez, A. Zamhuri, A. S. Walton, D. J. Tate, R. U. Khan, S. Aphichatpanichakul, A. B. Foster, S. Broll, M. L. Turner, *Adv. Sci.* **2020**, 2002010.
[11] Q. Meng, W. Hu, *Phys. Chem. Chem. Phys.* **2012**, *14*, 14152–14164.
[12] K. Liu, B. Ouyang, X. Guo, Y. Guo, Y. Liu, *npj Flexible Electronics* **2022**, 1–19, https://www.nature.com/npjflexelectron/articles?type=review-article.
[13] Y. Yu, Q. Ma, H. Ling, W. Li, R. Ju, L. Bian, N. Shi, Y. Qian, M. Yi, L. Xie, W. Huang, *Adv. Funct. Mater.* **2019**, *29*, 1904602.
[14] T. Schmaltz, G. Sforazzini, T. Reichert, H. Frauenrath, *Adv. Mater.* **2017**, *29*, 1605286.
[15] A. J. C. Kuehne, M. C. Gather, *Chem. Rev.* **2016**, *116*, 1–42.
[16] Y. Jiang, Y.-Y. Liu, X. Liu, H. Lin, K. Gao, W.-Y. Lai, W. Huang, *Chem. Soc. Rev.* **2020**, *49*, 5885–5944.
[17] M. M. Mróz, G. Sforazzini, Y. Zhong, K. S. Wong, H. L. Anderson, G. Lanzani, J. Cabanillas-Gonzalez, *Adv. Mater.* **2013**, *25*, 4347–4351.
[18] H. Dong, H. Zhu, Q. Meng, X. Gong, W. Hu, *Chem. Soc. Rev.* **2012**, *41*, 1754–1808.
[19] M. J. Marsella, T. M. Swager, *J. Am. Chem. Soc.* **1993**, *115*, 12214–12215.
[20] A. Giovannitti, C. B. Nielsen, J. Rivnay, M. Kirkus, D. J. Harkin, A. J. P. White, H. Sirringhaus, G. G. Malliaras, I. McCulloch, *Adv. Funct. Mater.* **2016**, *26*, 514–523.
[21] K. Sugiyasu, T. M. Swager, *Bull. Chem. Soc. Jpn.* **2007**, *80*, 2074–2083.
[22] Z. Ma, P. Chen, W. Cheng, K. Yan, L. Pan, Y. Shi, G. Yu, *Nano Lett.* **2018**, *18*, 4570–4575.
[23] X. Guo, M. Baumgarten, K. Müllen, *Prog. Polym. Sci.* **2013**, *38*, 1832–1908.
[24] J. Roncalli, *Macromol. Rapid Commun.* **2007**, *28*, 1761–1775.
[25] H. S. O. Chan, S. C. NG, *Prog. Polym. Sci.* **1998**, *23*, 1167–1231.
[26] D. Vonlanthen, A. Rudnev, A. Mishchenko, A. Käslin, J. Rotzler, M. Neuburger, T. Wandlowski, M. Mayor, *Chem. Eur. J.* **2011**, *17*, 7236–7250.
[27] D. A. Doval, M. D. Molin, S. Ward, A. Fin, N. Sakai, S. Matile, *Chem. Sci.* **2014**, *5*, 2819–2825.
[28] A. Bedi, A. M. Armon, Y. Diskin-Posner, B. Bogosalvsky, O. Gidron, *Nat. Commun.* **2022**, *13*, 451.
[29] C. Schaack, A. M. Evans, F. Ng, M. L. Steigerwald, C. Nuckolls, *J. Am. Chem. Soc.* **2022**, *144*, 42–51.
[30] A. Fin, A. V. Jentzsch, N. Sakai, S. Matile, *Angew. Chem. Int. Ed.* **2012**, *51*, 12736–12739; *Angew. Chem.* **2012**, *124*, 12908–12911.
[31] M. D. Molin, Q. Verolet, A. Colom, R. Letrun, E. Derivery, M. Gonzalez-Gaitan, E. Vauthey, A. Roux, N. Sakai, S. Matile, *J. Am. Chem. Soc.* **2015**, *137*, 568–571.
[32] M. D. Molin, S. Matile, *Org. Biomol. Chem.* **2013**, *11*, 1952–1957.
[33] W. Su, *Printed Electronics: Materials, Technologies and Applications*, 1st ed., Wiley-VCH, Weinheim, **2016**, Chapter 8.
[34] L. Yu, Y. Hu, J. Li, Z. Wang, H. Zhang, Y. Huang, Y. Lou, Y. Sun, X. Lu, H. Liu, Y. Zheng, S. Wang, X. Chen, D. Ji, L. Li, W. Hu, *J. Mater. Chem. C* **2022**, *10*, 8874–8880.
[35] C. Liu, H. Lin, S. Li, H. Xie, J. Zhang, D. Ji, Y. Yan, X. Liu, W. Lai, *Adv. Funct. Mater.* **2022**, *32*, 2111276.
[36] C. P. Harvey, J. D. Tovar, *Polym. Chem.* **2011**, *2*, 2699–2706.
[37] F. Stellacci, C. Bertarelli, F. Toscano, M. C. Gallazzi, G. Zotti, G. Zerbi, *Adv. Mater.* **1999**, *11*, 292–295.
[38] T. Kawai, Y. Nakashima, M. Irie, *Adv. Mater.* **2005**,*17*, 309–314.
[39] H. Cho, E. Kim, *Macromolecules* **2002**, *35*, 8684–8687.
[40] B. Jousselme, P. Blanchard, N. Gallego-Planas, J. Delaunay, M. Allain, P. Richomme, E. Levillain, J. Roncali, *J. Am. Chem. Soc.* **2016**, *125*, 2888–2889.
[41] B. Jousselme, P. Blanchard, M. Allain, E. Levillain, M. Dias, J. Roncali, *J. Phys. Chem.* **2006**, *110*, 3488–3494.
[42] V. A. Azov, J. Cordes, D. Schlüter, T. Dülcks, M. Böckmann, N. L. Doltsinis, *J. Org. Chem.* **2014**, *79*, 11714–11721.
[43] G. M. Peters, J. D. Tovar, *J. Am. Chem. Soc.* **2019**, *141*, 3146–3152.
[44] A. Peters, N. R. Branda, *Adv. Mater. Opt. Electron.* **2000**, *10*, 245–249.
[45] T. Kaieda, S. Kobatake, H. Miyasaka, M. Murakami, N. Iwai, Y. Nagata, A. Itaya, M. Irie, *J. Am. Chem. Soc.* **2002**, *124*, 2015–2024.

[46] T. Kawai, T. Sasaki, M. Irie, *Chem. Commun.* **2001**, *2010*, 711–712.
[47] N. Tanifuji, M. Irie, K. Matsuda, *Chem. Lett.* **2005**, *34*, 1580–1581.
[48] J. Maciejewski, A. Sobczuk, A. Claveau, A. Nicolai, R. Petraglia, L. Cervini, E. Baudat, P. Miéville, D. Fazzi, C. Corminboeuf, G. Sforazzini, *Chem. Sci.* **2017**, *8*, 361.
[49] L. Antolini, E. Tedesco, G. Barbarella, L. Favaretto, G. Sotgiu, M. Zambianchi, D. Casarini, G. Gigli, R. Cingolani, *J. Am. Chem. Soc.* **2000**, *122*, 9006–9013.
[50] Z. Yao, J. Wang, J. Pei, *Cryst. Growth Des.* **2018**, *18*, 7–15.
[51] R. S. Becker, J. S. de Melo, A. N. L. Macanita, F. Elisei, *J. Phys. Chem.* **1996**, *100*, 18683–18695.
[52] C. Bannwarth, E. Caldeweyher, S. Ehlert, A. Hansen, P. Pracht, J. Seibert, S. Spicher, S. Grimme, *WIREs Comput. Mol. Sci.* **2021**, *11*, e1493.
[53] S. Grimme, C. Bannwarth, P. Shushkov, *J. Chem. Theory Comput.* **2017**, *13*, 1989–2009.
[54] C. Bannwarth, S. Ehlert, S. Grimme, *J. Chem. Theory Comput.* **2019**, *15*, 1652–1671.
[55] Note: TDDFT calculations were executed on fully optimized, lowest-energy DFT (ωB97X-D/6-311 + G*) PTS trans conformers. The latter were initially obtained from a preliminary conformation screening based on the tight-binding DFT-based method GFN2-xTB (Geometry Frequency Non-covalent interactions-eXtended Tight Binding) coupled with meta-dynamics simulations with CREST (Conformer–Rotamer Ensemble Sampling Tool) algorithm; for details, see the Supporting Information.
[56] V. Hernandez, J. T. L. Navarrete, *J. Chem. Phys.* **1994**, *101*, 1369–1377.
[57] T.-J. Lin, S.-T. Lin, *Phys. Chem. Chem. Phys.* **2015**, *17*, 4127–4136.
[58] Note: For **PTS-T4**, ~83% of absorption intensity at 358 nm corresponds to ~74% of **PTS-T4.***trans*; for, ~79% of absorption intensity at 379 nm corresponds to ~71% of **PTS-T6.***trans*. Irradiation at 254 nm does not result in any isomerization of the olefin double from *trans* to *cis* (see the Supporting Information).
[59] N. Tamai, H. Miyasaka, *Chem. Rev.* **2000**, *100*, 1875–1890.
[60] H. H, Jaffé, S. Yeh, R. W. Gardner, *J. Mol. Spectrosc.* **1958**, *2*, 129–136.
[61] H. M. D. Bandara, S. C. Burdette, *Chem. Soc. Rev.* **2012**, *41*, 1809–1825.

Manuscript received: August 29, 2022
Accepted manuscript online: September 22, 2022
Version of record online: October 31, 2022